Fluorescent Copolymers for Bacterial Bioimaging and Viability Detection

Yang Si, Chloé Grazon, Gilles Clavier, Jutta Rieger, Yayang Tian, Jean-Frédéric Audibert, Bianca Sclavi, Rachel Méallet-Renault

Fluorescent copolymers for bacterial bioimaging and viability detection

Yang Si[a,b,†], Chloé Grazon[a], Gilles Clavier[a], Jutta Rieger[c], Yayang Tian[a], Jean-Frédéric Audibert[a], Bianca Sclavi[b,*, ‡], Rachel Méallet-Renault[a,*,§]

[a] Université Paris-Saclay, ENS Paris-Saclay, CNRS, PPSM, 91190, Gif-sur-Yvette, France.

[b] Université Paris-Saclay, ENS Paris-Saclay, CNRS, LBPA, 91190, Gif-sur-Yvette, France.

[c] Sorbonne Université, CNRS, Institut Parisien de Chimie Moléculaire, UMR 8232, Equipe Chimie des Polymères, 75252 Paris, France

KEYWORDS. bacteria, bioimaging, fluorescence, polymer, RAFT, flow cytometry, viability detection.

ABSTRACT: Novel fluorescent labels with high photostability and high biocompatibility are required for microbiological imaging and detection. Here, we present a Green Fluorescent Polymer Chain (GFPC), designed to be non-toxic and water-soluble, for multi-color bioimaging and real-time bacterial viability determination. The copolymer is synthesized using a straightforward one-pot RAFT polymerization technology. We show that GFPC does not influence bacterial growth and is stable over several hours in a complex growth medium and in the presence of bacteria. GFPC allows the labelling of bacterial cytoplasm for multi-color bacterial bioimaging applications. It can be used in combination with propidium iodide (PI) to develop a rapid and reliable protocol to distinguish and quantify, in real-time, by flow cytometry, live and dead bacteria.

Fluorescent labelling is one of the most common methodologies used for bioanalytical purposes.[1] Fluorescence techniques are considered to be very sensitive[2] since they can sense, in some cases, up to a single molecule.[3] Moreover, one of the most important advantages of fluorescence is its versatility.[4] There are a large number of different fluorescent materials and molecules, and still more are under development in order to meet the challenging requests for biological imaging (resolution, selectivity, specificity, targeting, brightness, stability…).

Different classes of materials are currently being developed and employed as fluorescent probes. They mainly include organic dyes,[1,2,5,6] fluorescent proteins,[7–10] fluorescent macromolecules[11–17] and quantum dots.[18–22] Nevertheless, organic dyes are still the most used,[23] certainly due to their small size, commercial availability, and the existence of standard protocols.

Nowadays, fluorescent materials with high levels of photostability[24] and biocompatibility[25,26] are more and more needed for life sciences imaging experiments. At the same time, recent developments in macromolecular synthesis protocols are bringing forward new materials with a great potential to solve some of the drawbacks associated with "standard" fluorophores, such as low levels of photostability[27,28] and water solubility.[4,29] Furthermore, these polymeric materials can now be functionalized in order to be more biocompatible and water-soluble, making them suitable for multi-color bioimaging uses.[30] The combination of these advanced features has made fluorescent polymeric materials an important and highly promising tool, either for fluorescence imaging and sensing, or for in vitro and in vivo[31] labeling of bacteria, cells,[17] tissues, and whole organisms.

Bacteria are the earliest and longest life forms on earth. They can inhabit every corner of the earth: water, soil, trees, human, animals and even nuclear waste.[31] An improved understanding of bacterial metabolism and physiology is important for medical research,[32,33] monitoring of water resources,[34,35] and in the food industry.[36,37]

Bioimaging applications of bacteria by different kinds of fluorescent labels have been developed intensively in recent years.[38–42] Especially, fluorescent proteins[43] are used to label bacterial cells and detect their movements, to study the changes of gene expression in real time[38] and other important characteristics such as the effects of overexpression of proteins, and the changes in cellular metabolism.[44–46] However, they tend to quickly photobleach and their relatively high molar mass (around 26-28kDa) may interfere with the function and localization of the labelled proteins as well as their interaction with other molecules.[1,2,28] Quantum dots have also been widely used for imaging applications in bacteria.[18–20] Dwarakanath et al. for example demonstrated that CdSe/ZnS QDs exhibit fluorescence emission blue shifts when conjugated to antibodies that are bound to bacteria.[47] Fluorescent CdSe/ZnS QDs were also used for super-resolution fluorescence microscopy on Shewanella oneidensis bacteria.[48] In comparison with traditional organic dyes, QDs are more photostable and

brighter, however, they are difficult to stabilize in water[49] and have been shown to be toxic[50]. Furthermore, blinking and complex fluorescence decays should be considered when developing fluorescent labels with QDs.[1] In contrast, fluorescent organic polymer nanoparticles have attracted great attention for applications related to fluorescent labelling in bacteria because of their high photostability, abundant surface modification, easy bioconjugation, and most importantly low toxicity for living systems.[51] Wang et al. demonstrated that organic polymeric materials can be used to coat the bacterial surface and form bacteria microparticles to perform multiplex biological imaging and analysis.[52] Bioconjugation of a nanoparticle surface with various biological functional groups such as streptavidin, biotin[53] and antibodies[54,55] also allows to target the bacterial surface for tracking the movements of bacteria,[56] for detection of bacteria and monitoring bacterial growth.[57] However, because of their size (>50nm) fluorescent nanoparticles are not suitable for internalization by live bacterial cells since only particles around a few nanometers can be transported into the cell by passive transport.[58] It seems thus important to design small fluorescent, water-soluble copolymer chains, which retain brightness, but are smaller than polymeric nanoparticles. As such they constitute a good compromise between organic dyes and polymeric nanoparticles, being able to enter bacteria allowing internal bioimaging.

In this work, we report the synthesis and full characterization of a random copolymer, named Green Fluorescent Polymer Chain (GFPC), which is water-soluble, biocompatible, non-toxic, stable and highly fluorescent. These features make it suitable for the development of microbiological applications such as labelling the bacterial cytoplasm for multi-color bioimaging applications and for rapid and reliable real-time detection of the viability of bacteria.

Results and Discussion

Synthesis and characterizations of the Green Fluorescent Polymer Chain (GFPC). The synthesis of the anionic green fluorescent polymer chain (GFPC) was performed using a reversible addition-fragmentation chain-transfer (RAFT) polymerization. This technique was selected as it allows the design of polymer chains with the desired molar mass, i.e. length, and to synthesize a batch of copolymer chains which is homogeneous in terms of comonomer distribution within the different chains. Three monomers, namely poly(ethylene oxide) methyl ether acrylate (APEG), acrylic acid (AA) and a methacrylate-functionalized BODIPY (BDπ, synthesized as described elsewhere[59]), were copolymerized in the presence of a trithiocarbonate RAFT agent (TTCA) (Figure 1A). After 10 hours, the copolymerization was stopped by immersion in iced water. The overall AA and APEG monomers conversion (80%) was determined by ^{1}H NMR in $CDCl_3$. The kinetic of AA and APEG conversion is shown in Table S1 and Figure S1B. The BDπ conversion (69%) was determined by SEC using UV-Vis detection (Figure S1, see SI for details). Monitoring of the copolymerization over time (Figure S1, Table S1) showed that the fluorescent monomer is randomly incorporated within the polymer chain. The final copolymer composition was determined as P(AA_7-*co*-$APEG_7$-*co*-$BD\pi_2$)-TTCA, and the number-average molar mass (Mn) determined by SEC was Mn = 4550 g mol^{-1} for a low molar mass dispersity (Đ) of 1.27.

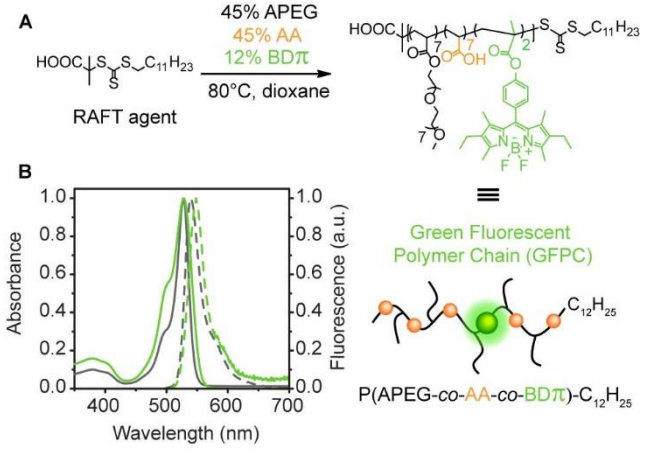

Figure1. A: synthesis of GFPC *via* RAFT polymerization; B: absorption (full lines) and fluorescence emission (dotted lines, λ_{exc} = 495nm) normalized spectra of BDπ monomer (black) in toluene and GFPC (green) in water (pH = 7.0).

The GFPC was designed to be negatively charged in water at pH=7, thanks to the carboxylates functions (COOH/COO^-, pKa~4-5) introduced by the AA in the copolymer. As expected, the zeta potential (ζ) of GFPC is strongly negative (-38.4±0.8mV) as recorded in distilled water at 25°C, due to the carboxylates moieties.

Fluorescence and absorption spectroscopy analysis of GFPC are displayed in Figure 1C and their main spectroscopic data are given in Table 1. The BDπ monomer in toluene shows the expected absorption spectrum for a BODIPY fluorophore[60] with an intense band in the visible region located at 528 nm (corresponding to a π→π* transition) and a vibrational shoulder at higher energy. A second, less intense band is located in the UV region at around 380 nm. The maximum of fluorescence emission is found at 540 nm, exhibiting a Stokes Shift of 421cm^{-1} (12 nm).

The GFPC in water shows the same maximum absorption at 528 nm as the monomer (BDπ). Nevertheless, the absorption band of the polymer chains in water is larger than the monomer (Full Width at Half Maximum, FWHM 1745 cm^{-1} vs 868 cm^{-1}). Such band broadening (on both band edges) has already been observed when BODIPY dyes are confined in a polymer matrix and/or in an aggregated state.[61,62] Absorption and emission spectra of cascade concentrations of GFPC in water have been measured (Figure S2), the FWHM stays the same over the several concentrations, indicating a uni-level homogenous distribution of GFPC in water. Moreover, the hydrodynamic diameter of GFPC from 2.2×10^{-4} M to 4.4×10^{-5} M were measured, both in water at 20°C and in LB growth media at 37°C (Figure S3). In both cases, whatever the concentration, there is no significant change in the hydrodynamic diameter (D_h ~ 7 nm). Therefore, GFPC presumably adopts a folded, unimolecular micellar structure with the hydrophilic groups

pointing outward and the hydrophobic BODIPY moieties aggregated inward minimizing thereby their contact with water. A red shift of the fluorescence emission (8 nm) is observed between the free monomer in toluene and GFPC in water, while the bandwidth is similar (996 cm^{-1} vs 950 cm^{-1}). The Stokes Shift of the polymer (691 cm^{-1}, 20 nm) is slightly higher than the monomer (421 cm^{-1}, 12 nm). The excitation spectra for GFPC and the BDπ monomer virtually superimpose with their respective absorption spectra (Figure S4B), showing that all absorbing species contribute to emission.

Table1. Main spectroscopic properties of BDπ and GFPC

Sample	Solvent	λ_{abs} /nm	$FWHM_{abs}$ /cm^{-1}	λ_{em} /nm	$FWHM_{em}$ /cm^{-1}	ϕ_F /%[a]	B /$M^{-1}cm^{-1}$[b]
BDπ	toluene	528	868	540	950	70	51100
GFPC	water	528	1745	548	966	20	29200
GFPC	toluene	528	906	542	943	74	108040

[a]Error of 15%[62], [b]Brightness determined by Equation S3.

In water, the fluorescence quantum yield of GFPC is 20%, while the one of BDπ monomer in toluene is 70%. Altogether, those spectroscopic observations of GFPC (red shift, Stokes-shift, decrease of quantum yield), are in agreement with the aggregation of BDπ due to the "folded" conformation of the polymer chain in water, stabilized by the carboxylates and PEG moieties. To confirm this hypothesis, GFPC was analyzed in toluene, where the polymer is in a favorable solvent and consequently the chain unfolded (Figure S5). The absorption and fluorescence spectra of GFPC in toluene are identical to the ones of BDπ and the fluorescence quantum yield recover its initial value (74%) (Table 1).

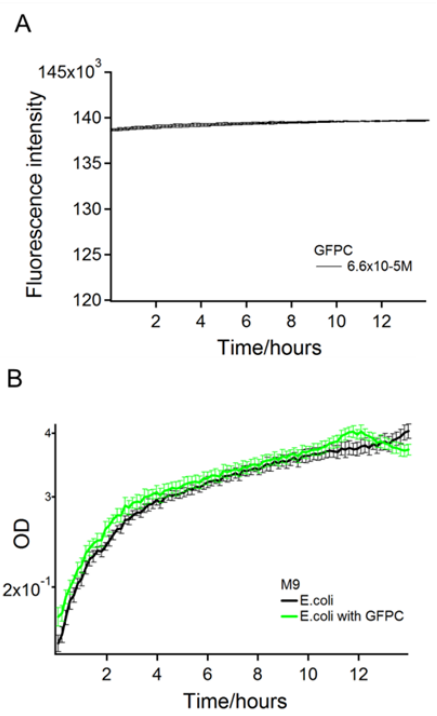

Figure2. A: evolution of fluorescence intensity of GFPC ([GFPC] =6.6 $\times 10^{-5}$ M) overnight (37°C, M9 Minimal Medium). The error bars indicate the difference between the three technical replicates from the same plate (<1.3%); **B**: growth curves of E.coli bacteria alone (black lines) and incubated with GFPC (green lines) at 6.6×10^{-5}M in M9 minimal medium overnight. The error bars indicate the difference between the three technical replicates from the same plate (<6.6%).

GFPC stability. In order to assess the stability of GFPC, the fluorescence intensity of GFPC was monitored overnight ([GFPC] = 6.6×10^{-5}M). GFPC was incubated in M9 minimal medium in a plate reader at 37°C in the measurement chamber for 14 hours. During this observation time, the fluorescence intensity of GFPC remained practically constant (Figure 2A), showing their very good stability in these experimental conditions.

Toxicity assessments of GFPC on *E.coli* growth. In order to assess the toxic effect of GFPC on E.coli, their growth rates were measured in the presence and absence of GFPC in M9 minimal medium by absorbance measurements (OD@600nm). The GFPC concentration used was 6.6×10^{-5}M (Figure 2B). Over ten hours of incubation, the growth curves of bacteria with and without GFPC were essentially identical. This means that GFPC has no toxicity effect on bacterial growth on a long-time scale.

Bioimaging of E.coli labelled with GFPC. *E.coli*'s interaction with GFPC was measured by wide field epifluorescence microscopy. The fluorescence images of *E.coli* alone (Figure 3A1) show the auto-fluorescence of the E.coli cells. GFPC solutions were added to the E.coli suspension to reach final concentrations of 6.6×10^{-5} M. After one hour incubation of *E.coli* with GFPC at 37°C, samples are washed three times with PBS before observation under microscope. All the cells show intense green light emission (Figure 3A2, Figure S6).

GFPC can thus label *E.coli* bacteria efficiently. When zooming on individual cells, an inhomogeneous distribution of the fluorescence intensity was observed within the bacteria (Figure 3A3). We hypothesized that since GFPC is anionic it can only reside in the bacterial cytoplasm without interacting with the negatively charged DNA. In order to test this assumption a red fluorescent, cell-permeable DNA stain, DRAQ 5, was co-incubated with the GFPC and the bacterial cells.

DRAQ5 (5×10^{-6}M) was added at the same time as GFPC (6.6×10^{-5}M) to an *E.coli* suspension in M9 medium and incubated for one hour. Samples were washed three times with PBS before observation under microscope (Figure 3B).

The green fluorescence of GFPC (Figure 3B2), and the red emission of DRAQ5 (Figure 3B3) were recorded independently. After overlapping the images in Figure3 B and C, it appears clearly that the red and green emissions do not overlap with each other (Figure 3B4). This indicates that GFPC could label the bacterial cytoplasm but not the DNA.

A cell membrane labeling dye, PKH26 (2×10^{-6}M), was also co-incubated with GFPC to further test its applicability in multi-color bioimaging of bacteria. Again the bacterial cytoplasm was stained by GFPC (6.6×10^{-5}M) (Figure 3C2) and the membrane was labelled by PKH26 (Figure 3C3). The overlap of the two images shows that the fluorescence of PKH26 and GFPC are not influenced by each other (Figure 3C4). GFPC is thus compatible with different types of commercial dyes for multi-color imaging.

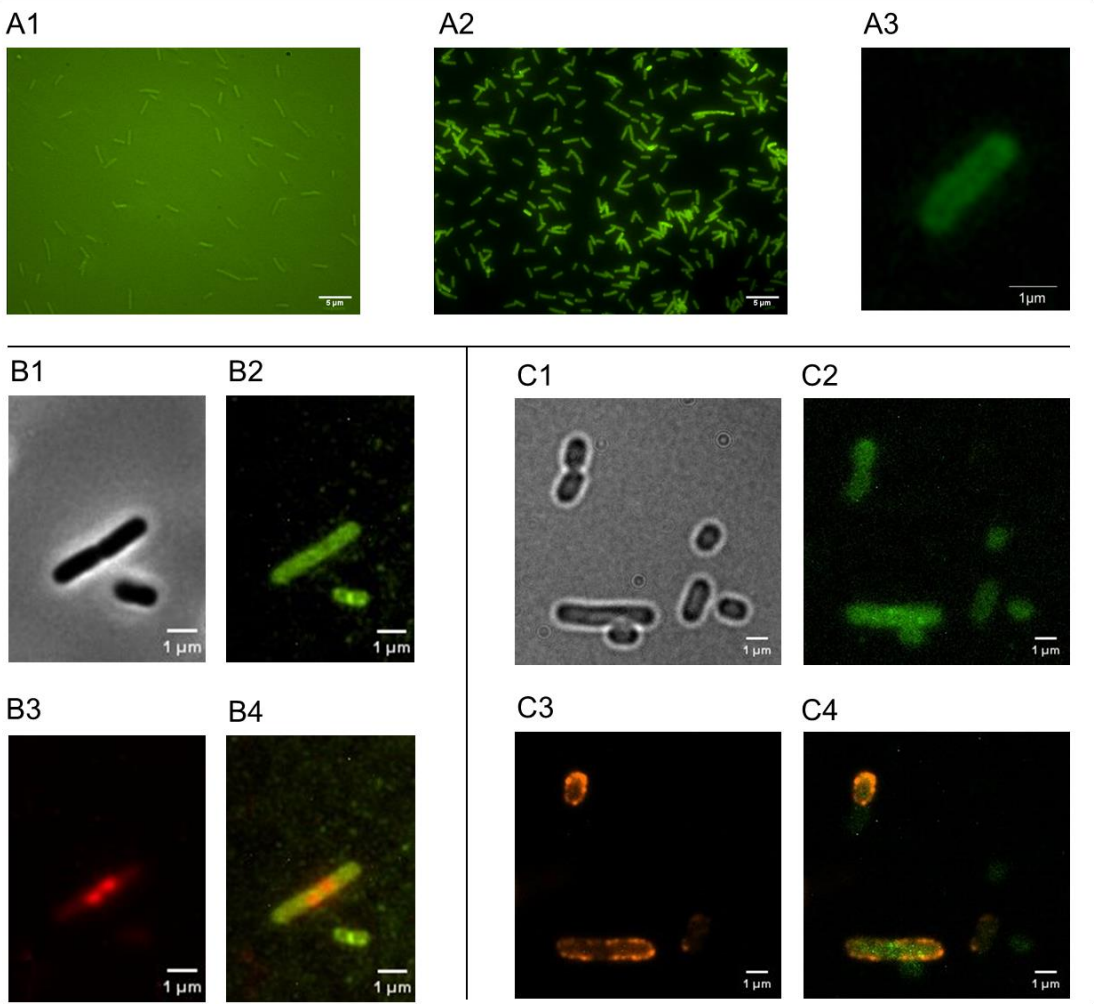

Figure3. A: fluorescence images of *E.coli* alone (A1) and *E.coli* labelled with GFPC (A2). A3 is a zoom of one bacterium from image A2. **B**: phase contrast image of *E.coli* bacteria (B1). Fluorescence images of *E.coli* labelled with GFPC and DRAQ5 in the green (B2) and red (B3) channel respectively. B4: Overlap of images B2 and B3. **C**: Bright field image of *E.coli* bacteria (C1). Fluorescence images of *E.coli* labelled with GFPC and PKH26 in the green (C2) and red (C3) channel. C4: Overlap of images C2 and C3.

GFPC for detection and quantification of live/dead bacteria by flow cytometry. Accurate measurements of live, dead, and total bacteria are very important in microbiology applications.[63] The traditional way to determine the viability of bacteria is to measure their ability to form colonies on solid growth medium or to proliferate in liquid nutrient broths.[64,65] Culture-based methods are time-consuming[66] and difficult to apply to slow growing or viable, but non-culturable organisms. More importantly, the traditional tests don't provide real-time information which is

needed in industrial manufacturing.[67] Flow cytometry is a technique which was first used on eukaryotic cells, but that has also been applied to measurement of viability, metabolic mechanisms, and antigenic markers of bacteria.[68]

Because of their intact membranes and cell walls, live bacteria are impermeable to dyes such as propidium iodide (PI) which can only stain cells with damaged membranes. GFPC is permeant and can label all cells, live and dead. As a result, GFPC in combination with PI, which emits in the red, could provide a rapid and reliable real-time method to distinguish and quantify live and dead bacteria in flow cytometry experiments.

In biological experiments, sample preparation steps such as a wash step, can lead to osmotic shock and result in cell death. We cultured E.coli bacteria in the presence of GFPC at 37°C in the dark for one hour. The cells were then subjected to six wash steps to provoke cell death before adding propidium iodide. The sample was subsequently analyzed by flow cytometry (Figure 4).

As expected, the total bacterial population demonstrated strong green fluorescence from the GFPC in the FL1 channel (99%, see R3-R4 zones in Figure 4A, B), independently of whether they were dead or alive. The dead population showed both the green GFPC emission in the FL1 channel and the strong red fluorescence from PI in the FL2 channel (see R4 zone in Figure 4A, C) and accounted for 18% of the total population. The viable bacterial population (81%) demonstrated weak red fluorescence and intense green emission (see R3 zone in Figure 4A, C). The viability can thus be measured by the proportion of cells stained by GFPC (total population) and PI (dead population). Thus, during our sample preparation, 18% of bacterial cells died because of the pressure introduced by the washing process.

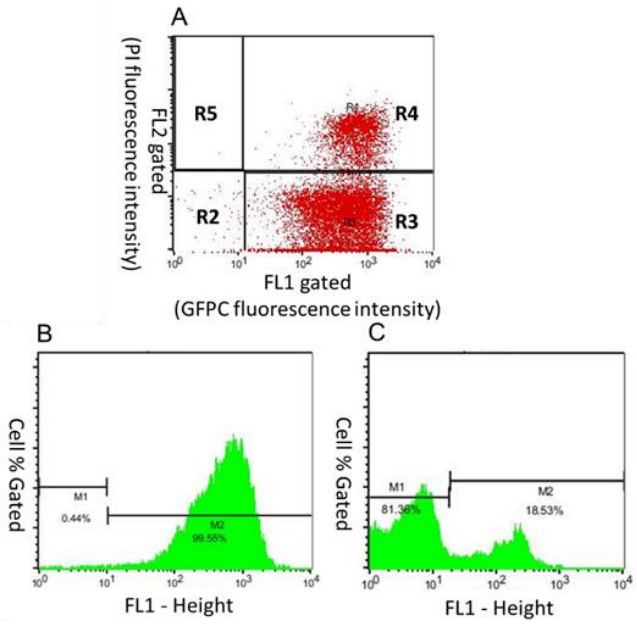

Figure4. A. Representative FL1 (GFPC) vs. FL2 (PI) dot plots of bacteria stained with GFPC and PI (R2: GFPC and PI negative cells; R3: GFPC positive, PI negative cells; R4: GFPC and PI positive cells; R5: GFPC negative, PI positive cells). **B.** Cell percentage with FL1 gated (GFPC). **C.** Cell percentage with FL2 gated (PI).

Compared to traditional methods, the one described here is less time-consuming.[66] Since it is more sensitive, this method can be applied to slow growing, or viable, but non-culturable organisms in diluted samples. The existing commercial kit (LIVE/DEAD™ BacLight™ Bacterial Viability Kit) uses the SYTO9 dye to stain the nucleic acids of all cells and PI to stain the nucleic acids of dead cells. The two dyes have the same target and may therefore interfere with each other resulting in erroneous results. The GFPC do not seem to interact with the nucleic acids, probably because of their net negative charge. The method described here provides a brand new strategy in developing real-time quantification of live/dead bacteria by flow cytometry by using GFPC to label the cytoplasm of all the cells and PI to stain the nucleic acids of dead bacteria with permeabilized membranes. This strategy avoids the interaction of the two dyes providing a rapid and reliable real-time method to distinguish and quantify live and dead bacteria.

Conclusions

A straightforward synthesis pathway to synthesize well-defined water-soluble fluorescent copolymers has been developed. Therefore, BODIPY-methacrylate (BDπ) was co-polymerized with water-soluble monomers, namely AA and APEG, using the reversible addition-fragmentation chain-transfer (RAFT) polymerization technology. A well-controlled, random copolymer was formed, composed as follows P(AA_7-*co*-$APEG_7$-*co*-$BD\pi_2$)-TTCA. This method is very simple, does not require the use of surfactants or other additives that may be detrimental for further biological applications of the sample. Furthermore, this method could be applied in the future to other polymerizable organic fluorescent dyes with minor synthetic efforts and no need for tedious purification steps.[69,70]

It was further shown that the novel fluorescent copolymer (GFPC) described herein has distinct features, including water solubility, stability in bacterial growth medium, nontoxicity, and biocompatibility. These features make them suitable for developments of microbiological applications such as labelling bacterial cytoplasm for multi-color bioimaging applications and for real-time detection of the viability in bacteria. The stable, nontoxic labeling of live cells could be used for cell tracking within tissues to study cell proliferation during infection for example. GFPC can label with high efficiency the bacterial cytoplasm but not nucleic acids, they have shown good compatibility with different types of commercial dyes (e.g. DRAQ5, PKH26, PI), and therefore GFPC can be used to develop multi-color bioimaging for bacteria. Due to their ability to label the cytoplasm of organisms and without toxic side effects, they could be used for labelling of bacteria and eukaryotic cells, as well as tissues.[71,72] At the same time, GFPC can provide a rapid and reliable real-time method to distinguish and quantify live and dead bacteria with a combination of propidium iodide (PI) by using flow cytometry. Moreover, the GFPC can be easily synthesized with low cost, and further

applied to introduce other dyes or building blocks into this copolymer backbone, which can be used in any laboratory without additional expensive instruments or operators.

Material and methods

Materials. Acrylic acid (99%, Sigma-Aldrich, AA), poly(ethylene oxide) methyl ether acrylate (Mn = 480 g.mol^{-1}, Sigma-Aldrich, APEG), 4,4'-azobis(4-cyanopentanoic acid) (Sigma-Aldrich, ACPA), 1,4-dioxane (anhydrous, 99.8%, Sigma-Aldrich), 2-(dodecylthiocarbonothioylthio)-2-methylpropionic acid (> 97%, Strem, TTCA), tetrahydrofuran (≥ 99.9%, Sigma-Aldrich), N,N-dimethylformamide (≥ 99.8%, Sigma-Aldrich, DMF), n-pentane (98%, Sigma-Aldrich), formaldehyde (36.5-38%, Sigma-Aldrich), DRAQ5 (BioStatus), PKH26 Red Fluorescent Cell Linker Kit for General Cell Membrane Labeling (Sigma-Aldrich), propidium iodide (Thermo Fisher Scientific) were used as received.

Synthesis of green fluorescent polymer chain (GFPC). BODIPY derivative: BODIPY methacrylate (BDπ) was synthesized as described elsewhere.[59] The green fluorescent polymer chain (GFPC) was synthesized in 1,4-dioxane at 80°C under nitrogen atmosphere. In a typical synthesis, APEG (0.9 mmol, 407 mg), AA (0.9 mmol, 65 mg), TTCA RAFT agent (0.1 mmol, 36.4 mg), DMF (0.54 mmol, 39.7 mg), BDπ (0.24 mmol, 113 mg) were dissolved in 0.97 mL of 1,4-dioxane at room temperature. Then, 0.03 mL of a 0.3 M solution of ACPA in 1.4-dioxane was added. The mixture solution was then purged with nitrogen for 30 min in an ice bath. After this, to initiate the polymerization, the mixture was placed in an oil bath and heated to 80°C. The reaction lasted for 10 hours and was stopped by putting the flask in iced water. The monomer conversion of AA and APEG was determined by ^{1}H-NMR in $CDCl_3$ by the relative integration of the internal reference peak of DMF at 8.0 ppm and the vinylic proton peaks of AA and APEG at 6.4, 6.1 and 5.8 ppm. After precipitation in n-pentane, a random fluorescent copolymer P(AA_7-*co*-$APEG_7$-*co*-$BD\pi_2$)-TTCA-C_{12}, named green fluorescent polymer chain (GFPC), was obtained with a number-average degree of polymerization (DPn) of 16 and an average number of 2 BODIPY fluorophores per chain. ^{1}H NMR: M_n = 4840 g mol^{-1} (see SI eq. S2). SEC: M_n = 4550 g mol^{-1}, Đ = 1.27, PS calibration.

Fluorescence spectroscopy. The UV-visible spectra were measured on a Varian Cary 5000 (Palo Alto, CA USA) double beam spectrometer using 4.5mL BRAND PMMA Cuvette. Corrected excitation and emission spectra were recorded on a SPEX Fluoromax-3 (Horiba Jobin-Yvon). A right-angle configuration was used. Optical density of the samples was measured to be less than 0.1 to avoid reabsorption artifacts. The relative fluorescence quantum yields Φ_F were measured using Rhodamine 590 (Φ_F = 0.95 in ethanol) as a reference (error of 15%).[59,73]

Size exclusion chromatography (SEC). The number-average molar mass M_n, weight-average molar mass M_w, and the molar mass distribution (dispersity Đ = M_w/M_n) were determined by size exclusion chromatography (SEC) using THF as an eluent at a flow rate of 1 mL min^{-1}. For analytical reasons, the carboxylic acidic functions of the copolymer were turned into methyl esters. After dissolution in a THF/H_2O mixture and acidification of the medium with a 1 M HCl solution, the copolymer is methylated using an excess of trimethylsilyldiazomethane. After filtration through 0.45 µm pore membrane, polymers were analyzed at a concentration of 5 mg mL^{-1} in THF. The SEC apparatus was equipped with a Viskotek VE 2100 automatic injector and two columns thermostated at 40 °C (PLgel Mixed; 7.5 mm × 300 mm; bead diameter = 5 µm). Detections were made with a differential refractive index detector (Viscotek VE 3580 RI detector) and an Ultraviolet–Visible (UV–vis) detector (Waters 486 tunable absorbance detector). The Viscotek OmniSEC software (v 4.6.2) was used for data analysis, and the relative M_n and Đ were calculated with a calibration curve based on polystyrene standards (from Polymer Laboratories).

Toxicity assessments of GFPC on the growth of *E.coli* Bacteria. Live *E.coli* bacterial cells (K-12 BW25113) were used for the following experiments. Bacterial cultures were prepared overnight from stock cultures inoculated in Luria Broth (LB) growth medium.

The overnight culture of bacteria was diluted 1:1000 in M9 minimal growth medium. 150 µL of this bacterial solution were placed in each well of a 96 well Falcon Polystyrene Flat Bottom Plate. The GFPC solutions were added into the E.coli solution to reach final concentration of 6.6×10^{-5}M. Each plate contained three repeats of the same concentration. One control with only bacteria and one blank with only M9 minimal medium were also prepared. 70 µL of mineral oil were added to each well in order to avoid evaporation. Samples were incubated in a plate reader (Perkin Elmer Victor3 1420 Multilabel Plate Counter) at 37°C in the measurement chamber. The growth of the cells was monitored every 9 minutes by reading the optical density (OD@600nm). Fluorescence was measured using a F485/14 filter for excitation and a F535/40 filter for emission. The experiments lasted for 14 hours.

Photostability assessment of GFPC. An overnight experiment was carried out to assess the photostability of GFPC. 150µL of the M9 minimal medium were placed in each well of a 96 well Falcon Polystyrene Flat Bottom Plate. The GFPC solutions were added into the solution to reach final concentration of 6.6×10^{-5}M. Each plate contained three repeats of the same concentration. One control with only the M9 minimal medium was also prepared. 70 µL of mineral oil were added to each well in order to avoid evaporation. Samples were incubated in a plate reader (Perkin Elmer Victor3 1420 Multilabel Plate Counter/ Tungsten-halogen lamp, 75 W) at 37°C in the measurement chamber. The fluorescence intensity of GFPC was measured every 9 minutes by using a F485/14 filter for excitation and a F535/40 filter for emission. The experiments lasted overnight for 14 hours.

Incubation to introduce GFPC into *E.coli* bacteria. 1mL of M9 minimal medium with an initial concentration of 5×10^7 CFU.mL^{-1} (OD=0.5) of *E.coli* bacteria was placed inside a 2mL Eppendorf Safe-Lock Tube. GFPC solutions

were added to this *E.coli* suspension to reach final concentrations of 6.6×10^{-5} M (0.3 mg.mL^{-1}). Two repeats of the same concentration were carried out during the experiments. The samples were incubated at 37°C in the dark for one hour. After the incubation, the cells were centrifuged at 4000 rpm for 3 minutes at 4°C and washed with PBS three times to remove free GFPC. The cells were then fixed with 4% formaldehyde at room temperature for 15 min, washed again with PBS for three times and re-suspended in PBS before flow cytometry measurements and bioimaging experiments.

GFPC for quantify live/dead bacteria by flow cytometry. Accurate quantitative measurements of live, dead, total bacteria and cells labeled with GFPC percentages were analyzed with a flow cytometer (BD, FACS Calibur; BD Biosciences) using the software BD CellQuest Pro.

Before flow cytometry, propidium iodide (PI, 10 µL, 1.3×10^{-2} mg.mL^{-1}) was added into each sample. Since PI emits in the red (617nm) once it is bound to the DNA inside the bacteria, it is screened by a FL3 (633nm) bandpass filter. On the other hand, GFPC emits in the green (548nm), so the emission signal is screened by a FL-1 (488 nm) bandpass filter. All instrument parameters were logarithmically amplified.

The voltage for forward scatter (FSC) and side scatter (SSC) were chosen so that the bacterial population was entirely on scale on an FSC vs. SSC plot. A non fluorescent bacterial sample was used to appropriately set the FL1 voltage. Individual FSC, SSC, FL1, FL3 histograms were checked to ensure that the bell-shaped populations are not cut off on the display. An event rate of ~1000 events per second was maintained to minimize the chance of coincidence and to improve population resolution. In the FSC vs. SSC plot, a live gate R1 was set around the bacterial population and a total of ~20,000 events inside the gate were measured.

DRAQ 5 for labelling the DNA of E.coli bacteria. DRAQ5 (5×10^{-6}M) was added at the same time with GFPC to E.coli suspension in M9 minimal medium. The samples were incubated at 37°C in the dark for one hour. After the incubation, the cells were gently centrifuged at 4000 rpm for 3 minutes at 4°C and washed with PBS three times to remove free GFPC and DRAQ5. The cells were then fixed with 4% formaldehyde at room temperature for 15 min. After the fixing process, cells were washed with PBS for three times and re-suspended in PBS before bioimaging experiments.

PKH26 for labelling the membrane of E.coli bacteria. The following procedure uses a 500 µL final staining volume containing final concentration of 2×10^{-6} M of PKH26 and 1×10^{8} cells.mL^{-1}. After introducing GFPC into E.coli bacteria, samples were washed three times by PBS and re-suspended in 250 µL diluent C (Sigma-Aldrich, an aqueous solution designed to maintain cell viability) in order to further perform membrane labelling. 1 µL PKH26 with an initial concentration of 1 mM was added into 250 µL diluent C, and then the bacterial solution was quickly transferred in to PKH26 dilution and mixed at room temperature for 5 minutes. The staining process is stopped by adding an equal volume of 1% BSA and incubate for 1 minute to allow binding of the dye in excess. Finally, the samples were washed three times by PBS and re-suspended in PBS before bioimaging experiments.

Fluorescence microscopy. Fluorescence images of GFPC, DRAQ5, PKH26 interacting with the E.coli bacteria were taken by epifluorescence microscopy (Nikon inverted microscope ECLIPSE TI-E with a motorized perfect focus system).

E.coli cells labelled with GFPC were illuminated with a white mercury lamp (Intensilight, NIKON) at 482nm/35nm (FITC-3540C BrightLine single-band filter, SEMROCK). E.coli cells labelled with DRAQ5 were illuminated at 632nm/22nm (BrightLine single-band filter, SEMROCK). E.coli cells labelled with PKH26 were illuminated at 543nm (TRITC-B BrightLine single-band filter, SEMROCK). The fluorescence was collected through a 536nm/40nm band-pass filter, a 695nm long-pass filter and a 593nm/40nm band-pass filter respectively and images were recorded with a 60× objective (CFI S Plan Fluor ELWD, NA 0.7) using an EM-CCD camera (Luca S, ANDOR).

Dynamic light scattering (DLS) measurements were performed with a Zetasizer Nano S90 from Malvern (90 ° angle, 5mW He-Ne laser at 633 nm, Nano DTS Software). The z-average particle diameter (Dz) of GFPC was measured at 20°C in milliQ water or at 37°C in LB (Luria broth) medium after filtration through a 0.45 µm membrane.

ASSOCIATED CONTENT

Supporting Information. The Supporting Information is available free of charge at http://pubs.acs.org.
Details of the characterizations of GFPC and BODIPY conversion; additional photophysical spectra and microscopy images

AUTHOR INFORMATION

Corresponding Author

* Bianca Sclavi – LCQB, CNRS UMR 7238, Sorbonne Université, 4 Place Jussieu, 75005 Paris, France ; *orcid.org/0000-0002-3883-8592; Email : bianca.sclavi@sorbonne-universite.fr*
*Rachel Méallet-Renault – Université Paris-Saclay, CNRS, ISMO, 91405, Orsay, France; *orcid.org/0000-0002-1083-6288*; rachel.meallet-renault@universite-paris-saclay.fr

Present Addresses

†: Epigenetic Chemical Biology, CNRS UMR3523, Institut Pasteur, 28 Rue du Dr Roux, 75015 Paris, France
‡: LCQB, CNRS UMR 7238, Sorbonne Université, 4 Place Jussieu, 75005 Paris, France
†: Université Paris-Saclay, CNRS, ISMO, 91405, Orsay, France.

Author Contributions

The manuscript was written through contributions of all authors. All authors have given approval to the final version of the manuscript.

Funding Sources

Financial support for this work was provided by the CNRS (Centre National de la Recherche Scientifique) of France–Interface Physique Chimie Biologie Soutien à la prise de risque–and by Institut d'Alembert (FR 3242 CNRS–ENS de Cachan). A PhD grant for Y.S. (01/10/2012 6466) and C.G. (01/10/2009 320) was provided by the MENESR (Ministère de l'Education Nationale, de l'Enseignement Supérieur et de la Recherche) of France.

ACKNOWLEDGMENT

ABBREVIATIONS

AA, Acrylic acid; ACPA, 4,4'-azobis(4-cyanopentanoic acid); APEG, Poly(ethylene oxide) methyl ether acrylate; BDπ, BODIPY methacrylate; BODIPY, 4,4-difluoro-4-bora-3a,4a-diaza-s-indacene; BSA, Bovine serum albumin; CFU, Colony-forming unit; DRAQ5, 1, 5-bis{[2-(di-methylamino)ethyl]amino}-4, 8-dihydroxyanthracene-9, 10-dione; E.coli, Escherichia coli; FSC, Forward scatter; FWHM, Full Width at Half Maximum; GFPC, Green Fluorescent Polymer Chain; LB, Luria Broth; PBS, Phosphate-buffered saline; PI, Propidium iodide; QDs, Quantum dots; RAFT, Reversible addition-fragmentation chain transfer; SSC, Side scatter; TTCA, 2-(dodecylthiocarbonothioylthio)-2-methylpropionic acid.

REFERENCES

(1) Valeur, B.; Berberan-Santos, M. N. *Molecular Fluorescence: Principles and Applications*, 2 edition.; Wiley-VCH: Weinheim, Germany, 2013.

(2) *Introduction to Fluorescence Sensing*; Demchenko, A. P., Ed.; Springer Netherlands: Dordrecht, 2009.

(3) Peterman, E. J. G.; Sosa, H.; Moerner, W. e. Single-Molecule Fluorescence Spectroscopy and Microscopy of Biomolecular Motors. *Annu. Rev. Phys. Chem.* **2004**, *55* (1), 79–96.

(4) Demchenko, A. P. *Advanced Fluorescence Reporters in Chemistry and Biology II: Molecular Constructions, Polymers and Nanoparticles*; Springer Science & Business Media, 2010.

(5) Li, B.; Lu, L.; Zhao, M.; Lei, Z.; Zhang, F. An Efficient 1064 Nm NIR-II Excitation Fluorescent Molecular Dye for Deep-Tissue High-Resolution Dynamic Bioimaging. *Angew. Chem. Int. Ed Engl.* **2018**, *57* (25), 7483–7487.

(6) Wu, D.; Chen, L.; Lee, W.; Ko, G.; Yin, J.; Yoon, J. Recent Progress in the Development of Organic Dye Based near-Infrared Fluorescence Probes for Metal Ions. *Coord. Chem. Rev.* **2018**, *354*, 74–97.

(7) Tsien, R. Y. The Green Fluorescent Protein. *Annu. Rev. Biochem.* **1998**, *67* (1), 509–544.

(8) Romei, M. G.; Boxer, S. G. Split Green Fluorescent Proteins: Scope, Limitations, and Outlook. *Annu. Rev. Biophys.* **2019**, *48* (1), 19–44.

(9) Scott, D. J.; Gunn, N. J.; Yong, K. J.; Wimmer, V. C.; Veldhuis, N. A.; Challis, L. M.; Haidar, M.; Petrou, S.; Bathgate, R. A. D.; Griffin, M. D. W. A Novel Ultra-Stable, Monomeric Green Fluorescent Protein For Direct Volumetric Imaging of Whole Organs Using CLARITY. *Sci. Rep.* **2018**, *8* (1), 1–15.

(10) Vetschera, P.; Mishra, K.; Fuenzalida-Werner, J. P.; Chmyrov, A.; Ntziachristos, V.; Stiel, A. C. Characterization of Reversibly Switchable Fluorescent Proteins in Optoacoustic Imaging. *Anal. Chem.* **2018**, *90* (17), 10527–10535.

(11) Adjili, S.; Favier, A.; Massin, J.; Bretonnière, Y.; Lacour, W.; Lin, Y.-C.; Chatre, E.; Place, C.; Favard, C.; Muriaux, D.; Andraud, C.; Charreyre, M.-T. Synthesis of Multifunctional Lipid–polymer Conjugates: Application to the Elaboration of Bright Far-Red Fluorescent Lipid Probes. *RSC Adv.* **2014**, *4* (30), 15569–15578.

(12) Bentolila, A.; Totre, J.; Zozulia, I.; Levin-Elad, M.; Domb, A. J. Fluorescent Cyanoacrylate Monomers and Polymers for Fingermark Development. *Macromolecules* **2013**, *46* (12), 4822–4828.

(13) Deng, H.; Su, Y.; Hu, M.; Jin, X.; He, L.; Pang, Y.; Dong, R.; Zhu, X. Multicolor Fluorescent Polymers Inspired from Green Fluorescent Protein. *Macromolecules* **2015**, *48* (16), 5969–5979.

(14) Henke, M.; Brandl, F.; Goepferich, A. M.; Tessmar, J. K. Size-Dependent Release of Fluorescent Macromolecules and Nanoparticles from Radically Cross-Linked Hydrogels. *Eur. J. Pharm. Biopharm. Off. J. Arbeitsgemeinschaft Pharm. Verfahrenstechnik EV* **2010**, *74* (2), 184–192.

(15) Jiang, R.; Huang, L.; Liu, M.; Deng, F.; Huang, H.; Tian, J.; Wen, Y.; Cao, Q.-Y.; Zhang, X.; Wei, Y. Ultrafast Microwave-Assisted Multicomponent Tandem Polymerization for Rapid Fabrication of AIE-Active Fluorescent Polymeric Nanoparticles and Their Potential Utilization for Biological Imaging. *Mater. Sci. Eng. C Mater. Biol. Appl.* **2018**, *83*, 115–120.

(16) Reisch, A.; Klymchenko, A. S. Fluorescent Polymer Nanoparticles Based on Dyes: Seeking Brighter Tools for Bioimaging. *Small* **2016**, *12* (15), 1968–1992.

(17) Thapaliya, E. R.; Zhang, Y.; Dhakal, P.; Brown, A. S.; Wilson, J. N.; Collins, K. M.; Raymo, F. M. Bioimaging with Macromolecular Probes Incorporating Multiple BODIPY Fluorophores. *Bioconjug. Chem.* **2017**, *28* (5), 1519–1528.

(18) Kloepfer, J. A.; Mielke, R. E.; Wong, M. S.; Nealson, K. H.; Stucky, G.; Nadeau, J. L. Quantum Dots as Strain- and Metabolism-Specific Microbiological Labels. *Appl. Environ. Microbiol.* **2003**, *69* (7), 4205–4213.

(19) Xue, X.; Pan, J.; Xie, H.; Wang, J.; Zhang, S. Fluorescence Detection of Total Count of Escherichia Coli and Staphylococcus Aureus on Water-Soluble CdSe Quantum Dots Coupled with Bacteria. *Talanta* **2009**, *77* (5), 1808–1813.

(20) Wu, S.-M.; Zhao, X.; Zhang, Z.-L.; Xie, H.-Y.; Tian, Z.-Q.; Peng, J.; Lu, Z.-X.; Pang, D.-W.; Xie, Z.-X. Quantum-Dot-Labeled DNA Probes for Fluorescence In Situ Hybridization (FISH) in the Microorganism Escherichia Coli. *ChemPhysChem* **2006**, *7* (5), 1062–1067.

(21) H. r, C.; Schiffman, J. D.; Balakrishna, R. G. Quantum Dots as Fluorescent Probes: Synthesis, Surface Chemistry, Energy Transfer Mechanisms, and Applications. *Sens. Actuators B Chem.* **2018**, *258*, 1191–1214.

(22) Gao, G.; Jiang, Y.-W.; Sun, W.; Wu, F.-G. Fluorescent Quantum Dots for Microbial Imaging. *Chin. Chem. Lett.* **2018**, *29* (10), 1475–1485.

(23) Resch-Genger, U.; Grabolle, M.; Cavaliere-Jaricot, S.; Nitschke, R.; Nann, T. Quantum Dots versus Organic Dyes as Fluorescent Labels. *Nat. Methods* **2008**, *5* (9), 763–775.

(24) Yogo, T.; Urano, Y.; Ishitsuka, Y.; Maniwa, F.; Nagano, T. Highly Efficient and Photostable Photosensitizer Based on BODIPY Chromophore. *J. Am. Chem. Soc.* **2005**, *127* (35), 12162–12163.

(25) Zhang, X.; Zhang, X.; Wang, S.; Liu, M.; Tao, L.; Wei, Y. Surfactant Modification of Aggregation-Induced Emission Material as Biocompatible Nanoparticles : Facile Preparation and Cell Imaging. *Nanoscale* **2013**, *5* (1), 147–150.

(26) Abdul Jalil, R.; Zhang, Y. Biocompatibility of Silica Coated NaYF4 Upconversion Fluorescent Nanocrystals. *Biomaterials* **2008**, *29* (30), 4122–4128.

(27) Kumar, C. S. S. R. *Nanomaterials for Biosensors*; John Wiley & Sons, 2007.
(28) Wang, F.; Tan, W. B.; Zhang, Y.; Fan, X.; Wang, M. Luminescent Nanomaterials for Biological Labelling. *Nanotechnology* **2006**, *17* (1), R1.
(29) Shi, Y.; Xu, D.; Liu, M.; Fu, L.; Wan, Q.; Mao, L.; Dai, Y.; Wen, Y.; Zhang, X.; Wei, Y. Facile Preparation of Water Soluble and Biocompatible Fluorescent Organic Nanoparticles through the Combination of RAFT Polymerization and Self-Polymerization of Dopamine. *J. Mol. Liq.* **2018**, *250*, 446–450.
(30) Yao, J.; Yang, M.; Duan, Y. Chemistry, Biology, and Medicine of Fluorescent Nanomaterials and Related Systems: New Insights into Biosensing, Bioimaging, Genomics, Diagnostics, and Therapy. *Chem. Rev.* **2014**, *114* (12), 6130–6178.
(31) Fredrickson, J. K.; Zachara, J. M.; Balkwill, D. L.; Kennedy, D.; Li, S. W.; Kostandarithes, H. M.; Daly, M. J.; Romine, M. F.; Brockman, F. J. Geomicrobiology of High-Level Nuclear Waste-Contaminated Vadose Sediments at the Hanford Site, Washington State. *Appl. Environ. Microbiol.* **2004**, *70* (7), 4230–4241.
(32) Lusby, P. E.; Coombes, A. L.; Wilkinson, J. M. Bactericidal Activity of Different Honeys against Pathogenic Bacteria. *Arch. Med. Res.* **2005**, *36* (5), 464–467.
(33) Finegold, S. M.; Jousimies-Somer, H. Recently Described Clinically Important Anaerobic Bacteria: Medical Aspects. *Clin. Infect. Dis.* **1997**, *25* (Supplement 2), S88–S93.
(34) Unc, A.; Goss, M. J. Transport of Bacteria from Manure and Protection of Water Resources. *Appl. Soil Ecol.* **2004**, *25* (1), 1–18.
(35) McKeon, D. M.; Calabrese, J. P.; Bissonnette, G. K. Antibiotic Resistant Gram-Negative Bacteria in Rural Groundwater Supplies. *Water Res.* **1995**, *29* (8), 1902–1908.
(36) Leroy, F.; De Vuyst, L. Lactic Acid Bacteria as Functional Starter Cultures for the Food Fermentation Industry. *Trends Food Sci. Technol.* **2004**, *15* (2), 67–78.
(37) Gram, L.; Ravn, L.; Rasch, M.; Bruhn, J. B.; Christensen, A. B.; Givskov, M. Food Spoilage—interactions between Food Spoilage Bacteria. *Int. J. Food Microbiol.* **2002**, *78* (1–2), 79–97.
(38) Andersen, J. B.; Sternberg, C.; Poulsen, L. K.; Bjørn, S. P.; Givskov, M.; Molin, S. New Unstable Variants of Green Fluorescent Protein for Studies of Transient Gene Expression in Bacteria. *Appl. Environ. Microbiol.* **1998**, *64* (6), 2240–2246.
(39) Jung, J. H.; Lee, J. E. Real-Time Bacterial Microcolony Counting Using on-Chip Microscopy. *Sci. Rep.* **2016**, *6*, 21473.
(40) Motoyama, Y.; Yamaguchi, N.; Matsumoto, M.; Kagami, N.; Tani, Y.; Satake, M.; Nasu, M. Rapid and Sensitive Detection of Viable Bacteria in Contaminated Platelet Concentrates Using a Newly Developed Bioimaging System. *Transfusion (Paris)* **2008**, *48* (11), 2364–2369.
(41) Qi, G.-B.; Gao, Y.-J.; Wang, L.; Wang, H. Self-Assembled Peptide-Based Nanomaterials for Biomedical Imaging and Therapy. *Adv. Mater.* **2018**, *30* (22), 1703444.
(42) Jelinek, R. Bioimaging Applications of Carbon-Dots. In *Carbon Quantum Dots: Synthesis, Properties and Applications*; Jelinek, R., Ed.; Carbon Nanostructures; Springer International Publishing: Cham, 2017; pp 61–70.
(43) Chudakov, D. M.; Matz, M. V.; Lukyanov, S.; Lukyanov, K. A. Fluorescent Proteins and Their Applications in Imaging Living Cells and Tissues. *Physiol. Rev.* **2010**, *90* (3), 1103–1163.
(44) Miroux, B.; Walker, J. E. Over-Production of Proteins in Escherichia Coli: Mutant Hosts That Allow Synthesis of Some Membrane Proteins and Globular Proteins at High Levels. *J. Mol. Biol.* **1996**, *260* (3), 289–298.
(45) Geoffroy, M.-C.; Guyard, C.; Quatannens, B.; Pavan, S.; Lange, M.; Mercenier, A. Use of Green Fluorescent Protein To Tag Lactic Acid Bacterium Strains under Development as Live Vaccine Vectors. *Appl. Environ. Microbiol.* **2000**, *66* (1), 383–391.
(46) Tombolini, R.; Unge, A.; Davey, M. E.; Bruijn, F. J. de; Jansson, J. K. Flow Cytometric and Microscopic Analysis of GFP-Tagged Pseudomonas Fluorescens Bacteria. *FEMS Microbiol. Ecol.* **1997**, *22* (1), 17–28.
(47) Sulatha Dwarakanath, J. G. B. Quantum Dot-Antibody and Aptamer Conjugates Shift Fluorescence upon Binding Bacteria. *Biochem. Biophys. Res. Commun.* **2004**, *325* (3), 739–743.
(48) Gunsolus, I. L.; Hu, D.; Mihai, C.; Lohse, S. E.; Lee, C.; Torelli, M. D.; Hamers, R. J.; Murhpy, C. J.; Orr, G.; Haynes, C. L. Facile Method to Stain the Bacterial Cell Surface for Super-Resolution Fluorescence Microscopy. *Analyst* **2014**, *139* (12), 3174–3178.
(49) Peng, H.; Zhang, L.; Soeller, C.; Travas-Sejdic, J. Preparation of Water-Soluble CdTe/CdS Core/Shell Quantum Dots with Enhanced Photostability. *J. Lumin.* **2007**, *127* (2), 721–726.
(50) Hardman Ron. A Toxicologic Review of Quantum Dots: Toxicity Depends on Physicochemical and Environmental Factors. *Environ. Health Perspect.* **2006**, *114* (2), 165–172.
(51) Yang, Y.; Wang, X.; Cui, Q.; Cao, Q.; Li, L. Self-Assembly of Fluorescent Organic Nanoparticles for Iron(III) Sensing and Cellular Imaging. *ACS Appl. Mater. Interfaces* **2016**, *8* (11), 7440–7448.
(52) Feng, X.; Yang, G.; Liu, L.; Lv, F.; Yang, Q.; Wang, S.; Zhu, D. A Convenient Preparation of Multi-Spectral Microparticles by Bacteria-Mediated Assemblies of Conjugated Polymer Nanoparticles for Cell Imaging and Barcoding. *Adv. Mater.* **2012**, *24* (5), 637–641.
(53) Pulkkinen, M.; Pikkarainen, J.; Wirth, T.; Tarvainen, T.; Haapa-aho, V.; Korhonen, H.; Seppälä, J.; Järvinen, K. Three-Step Tumor Targeting of Paclitaxel Using Biotinylated PLA-PEG Nanoparticles and Avidin–biotin Technology: Formulation Development and in Vitro Anticancer Activity. *Eur. J. Pharm. Biopharm.* **2008**, *70* (1), 66–74.
(54) Yang, J.; Lee, C.-H.; Park, J.; Seo, S.; Lim, E.-K.; Song, Y. J.; Suh, J.-S.; Yoon, H.-G.; Huh, Y.-M.; Haam, S. Antibody Conjugated Magnetic PLGA Nanoparticles for Diagnosis and Treatment of Breast Cancer. *J. Mater. Chem.* **2007**, *17* (26), 2695–2699.
(55) Fujita, Y.; Taguchi, H. Current Status of Multiple Antigen-Presenting Peptide Vaccine Systems: Application of Organic and Inorganic Nanoparticles. *Chem. Cent. J.* **2011**, *5* (1), 48.
(56) Fernandes, R.; Zuniga, M.; Sassine, F. R.; Karakoy, M.; Gracias, D. H. Enabling Cargo-Carrying Bacteria via Surface Attachment and Triggered Release. *Small* **2011**, *7* (5), 588–592.
(57) Si, Y.; Grazon, C.; Clavier, G.; Rieger, J.; Audibert, J.-F.; Sclavi, B.; Méallet-Renault, R. Rapid and Accurate Detection of Escherichia Coli Growth by Fluorescent pH-Sensitive Organic Nanoparticles for High-Throughput Screening Applications. *Biosens. Bioelectron.* **2016**, *75*, 320–327.
(58) Luo, P. G.; Stutzenberger, F. J. Nanotechnology in the Detection and Control of Microorganisms. *Adv. Appl. Microbiol.* **2008**, *63*, 145–181.
(59) Grazon, C.; Rieger, J.; Méallet-Renault, R.; Clavier, G.; Charleux, B. One-Pot Synthesis of Pegylated Fluorescent

Nanoparticles by RAFT Miniemulsion Polymerization Using a Phase Inversion Process. *Macromol. Rapid Commun.* **2011**, *32* (9–10), 699–705.
(60) Loudet, A.; Burgess, K. BODIPY Dyes and Their Derivatives: Syntheses and Spectroscopic Properties. *Chem. Rev.* **2007**, *107* (11), 4891–4932.
(61) Grazon, C.; Rieger, J.; Charleux, B.; Clavier, G.; Méallet-Renault, R. Ultrabright BODIPY-Tagged Polystyrene Nanoparticles: Study of Concentration Effect on Photophysical Properties. *J. Phys. Chem. C* **2014**, *118* (25), 13945–13952.
(62) Vu, T. T.; Dvorko, M.; Schmidt, E. Y.; Audibert, J.-F.; Retailleau, P.; Trofimov, B. A.; Pansu, R. B.; Clavier, G.; Méallet-Renault, R. Understanding the Spectroscopic Properties and Aggregation Process of a New Emitting Boron Dipyrromethene (BODIPY). *J. Phys. Chem. C* **2013**, *117* (10), 5373–5385.
(63) Davey, H. M.; Kell, D. B. Flow Cytometry and Cell Sorting of Heterogeneous Microbial Populations: The Importance of Single-Cell Analyses. *Microbiol. Rev.* **1996**, *60* (4), 641–696.
(64) Winslow, C.-E. A.; Brooke, O. R. THE VIABILITY OF VARIOUS SPECIES OF BACTERIA IN AQUEOUS SUSPENSIONS. *J. Bacteriol.* **1927**, *13* (4), 235–243.
(65) Nassif, N.; Coiffier, A.; Coradin, T.; Roux, C.; Livage, J.; Bouvet, O. Viability of Bacteria in Hybrid Aqueous Silica Gels. *J. Sol-Gel Sci. Technol.* **2003**, *26* (1–3), 1141–1144.
(66) Lazcka, O.; Del Campo, F. J.; Muñoz, F. X. Pathogen Detection: A Perspective of Traditional Methods and Biosensors. *Biosens. Bioelectron.* **2007**, *22* (7), 1205–1217.
(67) Josefsen, M. H.; Löfström, C.; Hansen, T. B.; Christensen, L. S.; Olsen, J. E.; Hoorfar, J. Rapid Quantification of Viable Campylobacter Bacteria on Chicken Carcasses, Using Real-Time PCR and Propidium Monoazide Treatment, as a Tool for Quantitative Risk Assessment. *Appl. Environ. Microbiol.* **2010**, *76* (15), 5097–5104.
(68) Nebe-von-Caron, G.; Stephens, P. J.; Hewitt, C. J.; Powell, J. R.; Badley, R. A. Analysis of Bacterial Function by Multi-Colour Fluorescence Flow Cytometry and Single Cell Sorting. *J. Microbiol. Methods* **2000**, *42* (1), 97–114.
(69) Breul, A. M.; Hager, M. D.; Schubert, U. S. Fluorescent Monomers as Building Blocks for Dye Labeled Polymers: Synthesis and Application in Energy Conversion, Biolabeling and Sensors. *Chem. Soc. Rev.* **2013**, *42* (12), 5366–5407.
(70) Thielbeer, F.; Chankeshwara, S. V.; Bradley, M. Polymerizable Fluorescein Derivatives: Synthesis of Fluorescent Particles and Their Cellular Uptake. *Biomacromolecules* **2011**, *12* (12), 4386–4391.
(71) Johnson, M. B.; Criss, A. K. Fluorescence Microscopy Methods for Determining the Viability of Bacteria in Association with Mammalian Cells. *J. Vis. Exp. JoVE* **2013**, No. 79.
(72) Zhu, H.; Fan, J.; Du, J.; Peng, X. Fluorescent Probes for Sensing and Imaging within Specific Cellular Organelles. *Acc. Chem. Res.* **2016**, *49* (10), 2115–2126.
(73) Kubin, R. F.; Fletcher, A. N. Fluorescence Quantum Yields of Some Rhodamine Dyes. *J. Lumin.* **1982**, *27* (4), 455–462.

Table of contents graphic